ORIGINAL ARTICLE

lajss.org
Latin American Journal of Solids and Structures

www.lajss.org

Effects of Non-Structural Walls on Mitigating the Risk of Progressive Collapse of RC Structures

Ali Altheeb[a], Ibrahim M. H. Alshaikh[b]*, Aref Abadel[a], Moncef Nehdi[c], Hussam Alghamdi[a]

[a]Department of Civil Engineering, College of Engineering, King Saud University, Riyadh 11421, Saudi Arabia. E-mails: aaltheeb@ksu.edu.sa, aabadel@ksu.edu.sa, hsghamdi@ksu.edu.sa

[b]Civil Engineering Department, University of Science and Technology, Faculty of Engineering, Sana'a, Yemen.
E-mail: ibrahimalshaikh86@gmail.com

[c]Department of Civil Engineering, McMaster University, Hamilton, ON, Canada. E-mail: nehdim@mcmaster.ca

* Corresponding author

https://doi.org/10.1590/1679-78257023

Abstract

This study aims to investigate the effect of the infilled frames through various important parameters (i.e., the openings' percentage in infill walls - several columns on the first floor are removed - partial infilled) in the RC structures, subject to progressive collapse scenarios. To this end, 3D finite element models were constructed by using the software ABAQUS. Numerical and experimental results were compared to substantiate the finite element models' capability of simulating the experimental models' behavior of Al-Chaar et al. (2002) in an accurate manner. The results showed that there was good agreement between experimental and numerical results. Moreover, the results indicated that there was a significant effect, which cannot be neglected, on the progressive collapse resistance; the reduction ratios in vertical displacement at the regions removed columns can reach up to 80%.

Keywords

Progressive Collapse; Infill Walls; Reinforced Concrete Frame; Numerical Simulation; Mitigating Progressive Collapse; ABAQUS.

Graphical Abstract

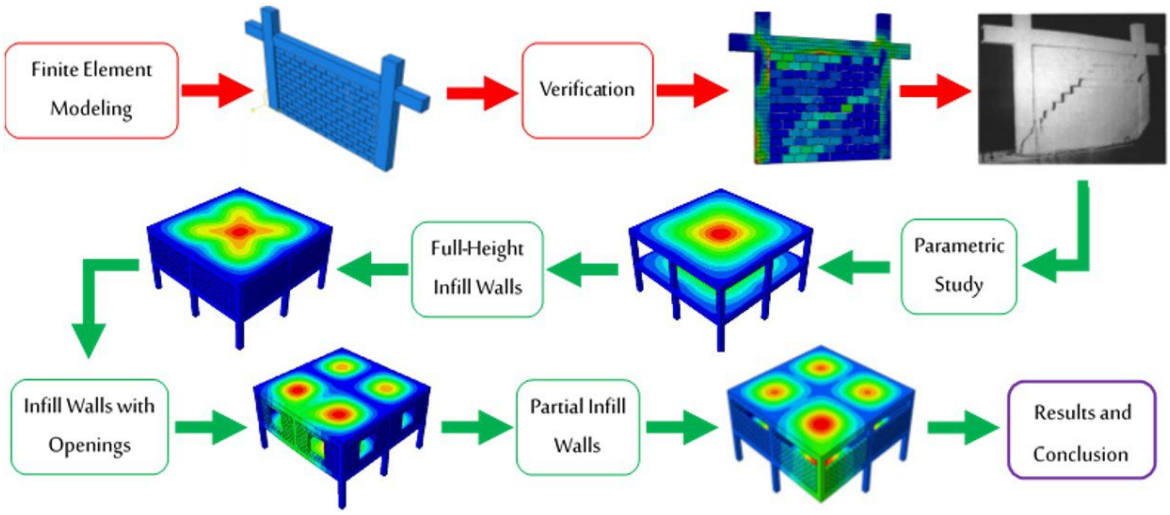

Received: March 12, 2022. In Revised Form: March 17, 2022. Accepted: March 24, 2022. Available online: March 25, 2022
https://doi.org/10.1590/1679-78257023

1 INTRODUCTION

In (ASCE 7-10), progressive collapse is referred to (ASCE, 2010) as an element-to-element failure spread, which results in either a full collapse or the collapse of a very extensive part of a given structure. Efforts were exerted over the last few decades to develop structures' design methods so that they can resist progressive collapse. Furthermore, considerable research on progressive collapse has been done. However, no substantial progress has been made except for several guidelines, which were set by organizations in the US like the DoD (2010) and GSA (2003). The most widespread and oldest structural systems are the masonry wall; they are still used for various purposes in structures. Also, the infill walls' effect is not considered in the general design code throughout the frames' design procedure; frames are fills in all cases (Daryan et al., 2009), whereby they consider such elements to be architectural, also non-structural elements (J. Centeno 2008, Lupoae et al., 2011). Infill walls intensify the frames' lateral stiffness. They are utilized to transfer interior horizontal forces and to allow an energy dissipation through a response to a non-linear for a number of deformation cycles (J. Centeno 2008). Generally, experimental tests are complicated, time-consuming, and costly to investigate the effects of the infill walls, especially with many different parameters. Currently, the numerical analysis is an applicable alternative to the experimental tests. Different numerical studies were conducted to simulate the behavior of masonry (Ibrahim AL-Shaikh, 2014, Abdulla et al., 2017, Shan et al., 2019). Few studies, however, were carried out to examine the possibilities of using infill walls for the progressive collapse in large-scale specimens. Shan et al. (2016), for instance, examined the impact of infilled walls on two one-third-scale, four-span, two-story RC frame structures' progressive collapse under scenarios of column removal using quasi-static loading. The results showed that infilled walls improved the resistance of progressive collapse. They acted as compressive struts, which produced alternate load paths for redistributing removal column loads. Researchers like (Li et al., 2016, Eren et al., 2019, Yu et al., 2019) carried out numerical studies by validating the numerical by holding a comparison with the experimental results of Shan et al. (2016). On the other hand, Sasani and Kropelnicki (2008) and Sasani (2008) conducted another experimental study to investigate a real six-story RC infilled-frame structure, subject to demolition by an explosion (2 columns were lost) to assess the building's response. In the experiment, the maximum vertical displacement is 6.4 mm; whereby progressive collapse did not take place. Also, the infilled walls were constraints, and they supported the beams when they carried further redistributed loads. In another study, Barros et al. (2019) examined the impact of non-structural infilled walls on the residential RC building's progressive collapse, which is subject to severe damage from a specific landslide. The authors conducted a numerical study using finite element methods, and they concluded that the infilled walls are important to restrain the damage due to the two-column removal. The collapse probability might reach 99% without the infilled walls. Thus, with these non-structural elements, increasing the structural robustness would approximately be 30%, and a corresponding collapse probability of 6%. Moreover, Qian et al. (2020a) conducted the tests of progressive collapse on the RC frames with/without the infill walls. Thus, the experimental studies investigated a series of five 1/4 scaled with two-bay and three-story. The results showed that infill walls can increase the first peak load by 256%, and even with 31% opening ratio, the infill walls might still intensify the first peak load by 88%.

According to previously conducted studies, the infilled walls can enhance the resistance of progressive collapse because they act as constraints and support the beams by carrying the additional redistributed loads (Sasani, 2008, Sasani and Kropelnicki, 2008, Shan et al., 2016, Barros et al., 2019, Qian et al., 2020a). Another advantage of the infilled walls involves attenuating the blast effects in the given column by a considerable reduction of the applied load. The walls can significantly reduce the blast pressure on the slab floors through acting like a shield (Woodson and Baylot, 2000). So far, many studies have been conducted and focused on full-height infill walls and sub-assemblage specimens testing (the impact of floor slabs, as well as the transverse beams, is neglected). However, there exists a noticeable lack of the existing information in the available literature regarding the infill walls with openings and partial infill walls, especially with 3D specimens under different column removal scenarios. In this paper, the finite element models are utilized to examine a series of fifteen 3D infilled RC frames, along with varied opening ratios, as well as partial infill under different scenarios of column removal. The modeling approach was carried out using ABAQUS software, which is illustrated in detail in the present work. The finite element models were substantiated by comparing the numerical and experimental results from Al-Chaar et al. (2002). This work aims to help researchers and structural engineers understand the contribution of the infill walls in various situations (i.e., even with gaps and openings) in developing the resistance of the progressive collapse of RC frames and, consequently, consider the effect of the infill walls during the design procedure in the existing design guidelines.

2 Details of the 3-D studied structure

In Sana'a, Yemen, one existing RC structure has been selected for analysis in this study. The location of the selected RC building is in a non-seismic zone; it consists of a ground floor and two other floors. The structural system involves ordinary frames. The RC structure was designed and detailed according to the ASCE 7-10 (ASCE, 2010) and ACI 318M-11 (ACI, 2011) for the Seismic Design Category "A" requirements. The building footprint is 2 bays by 2 bays (Figure 1). The heights of all floors are 3 m. The distance between column centerlines is 5.1 m (bay widths) for both orthogonal directions. Considering the standards' requirements and the vertical applying loads, the typical dimensions of square columns and dropped beams are 400 mm deep by 400 mm wide and 500 mm deep by 200 mm wide, respectively on the entire floors. The floor is a two-way solid RC slab with a thickness of 150 mm. In Figure 1 and Table 1, the details of the reinforcement and various structural elements' concrete dimensions are illustrated as follows:

Table 1. Details of the various structural elements

Slab Details		Beam Details		Column Details	
Dimensions (h)*	**Reinforcement**	**Dimensions (b × h) ***	**Reinforcement**	**Dimensions (b × h) ***	**Reinforcement**
150	• 7Ø12 mm/m for both directions.	200 × 500	• 3Ø16 mm top and bottom for external beams. • 4Ø16 mm top and 3Ø16 mm bottom for internal beams. • Ø8 mm stirrups @ 200 mm o.c.	400 × 400	• 8Ø16 mm main steel. • Ø8 mm ties @ 250 mm o.c.

* b = width of section; h = depth of section; all dimensions in mm.

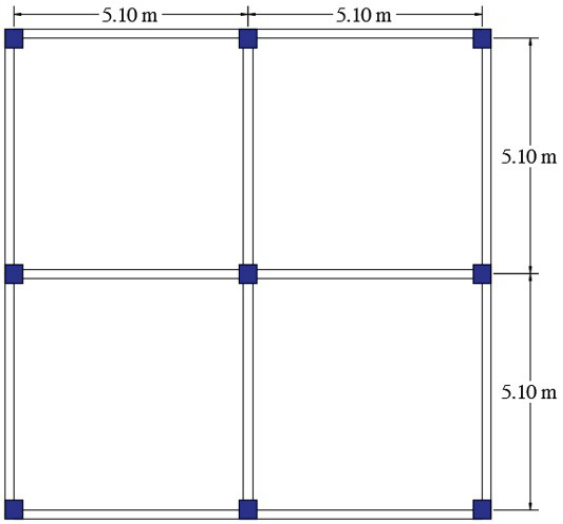

Figure 1. Dimensions of reinforced concrete buildings.

3 Finite Element Simulation/ Simulation Technique

The numerical simulation has proved superiority in the field of progressive collapse, especially with large-scale specimens that must be tested. In the numerical analysis of the 3-D structure's behavior, the ABAQUS (ABAQUS, 2012) commercial finite element software has been utilized. The ABAQUS package contains numerously varied element types. These are characterized according to the aspects, which describe the behavior. In this study, the first type of elements is a three-dimensional eight-node reduced integration element (C3D8R), which was used to model the concrete parts (i.e., columns, beams, slabs, and masonry units), whereas the second type of elements is truss elements, three-dimensional two-node (T3D2), which was used to model the reinforcing rebars.

3.1. Material models

The mechanical properties of concrete members (i.e., columns, beams, and concrete masonry unit) and reinforcing rebars were considered depending on the experimental results, which were conducted by Al-Chaar et al. (2002). However, some missing properties were calculated based on relevant design codes and the ABAQUS user's manual (ABAQUS, 2012). Table 2 illustrates the concrete, reinforcing rebars, and the concrete masonry properties of specimens tested by Al-Chaar et al. (2002).

Table 2. Concrete, reinforcing rebars, and concrete masonry properties (Al-Chaar et al., 2002)

Concrete (MPa)		Reinforcing Rebars (MPa)		Concrete masonry unit (MPa)
Compressive Stress (σ_c')	Young's modulus (E_o)	Yield Stress (σ)	Young's modulus (E)	Compressive Stress (σ_c')
38.438	29,992	338.5	200,000	12.907

The plasticity for concrete behavior has been applied in ABAQUS by utilizing the concrete damage plasticity (CDP) model for simulating the concrete behavior in beams, columns, and the concrete masonry unit. CDP followed Lubliner et al. proposed models (Lubliner et al., 1989), in addition to Lee and Fenves (1998). This model can simulate the behavior of each compressive strength, as well as the tensile strength of concrete, which is exposed to external pressures.

The compressive stress-strain (σ_c - ε_c) curves were obtained following Eurocode 2 (EN-1992-1-1, 2005a) provisions as shown in Figure 2. This relationship is described in Eq. (1), (2), (3), and (4) (EN-1992-1-1, 2005a). The concrete strains at maximum stress (ε_{c1}) were assumed as 0.0017 and 0.0025 for concrete members and concrete masonry unit, respectively, while 0.0035 for the maximum strain at failure (ε_{cu1}) for all concrete parts. The resulting relationship between σ_c and ε_c for concrete members and concrete masonry unit is shown in Figure 3. In this study, the CDP parameters, which are used to simulate concrete in ABAQUS, are shown in Table 3.

$$\sigma_c = \sigma_c' \frac{k\eta - \eta^2}{1+(k-2)\eta} \tag{1}$$

$$\eta = \frac{\varepsilon_c}{\varepsilon_{c1}} \tag{2}$$

$$\varepsilon_{c1} = 0.0007{\sigma_c'}^{0.31} \tag{3}$$

$$k = 1.05E_o\, {\varepsilon_{c1}}/{\sigma_c'} \tag{4}$$

where σ_c is the compressive stress, k is the material coefficient, and η is the strain coefficient.

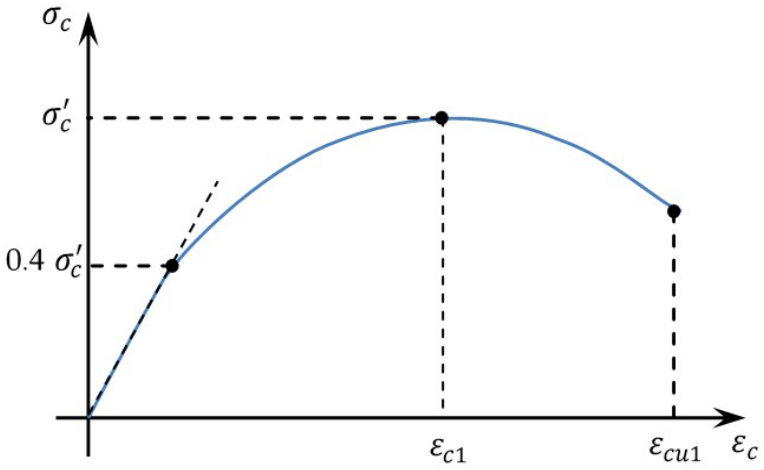

Figure 2. Representing the schematic of the compressive stress-strain curve for structural analysis ($0.4\sigma_c'$ used to define the approximate value of E_o) (EN-1992-1-1, 2005a).

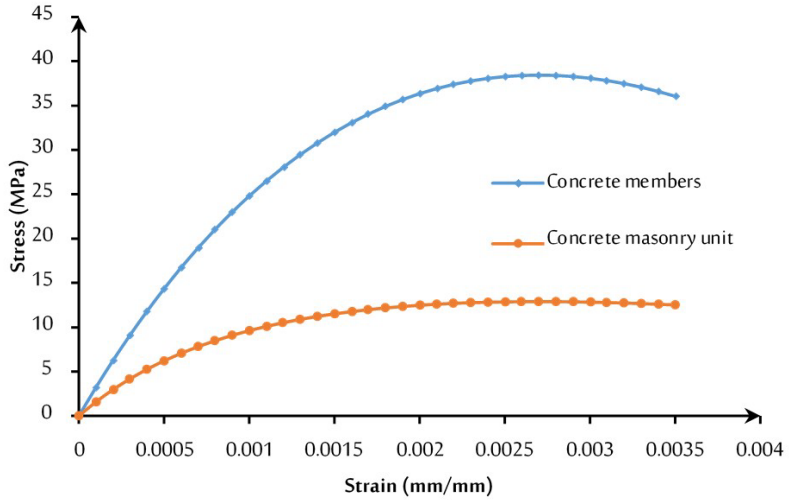

Figure 3. The stress-strain curve of concrete in compression.

Table 3. Concrete implemented material parameters in this study

Parameter	Value	Definition	Denotation
ϵ	0.1	Flow potential eccentricity	(ABAQUS, 2012)
ψ	35	Dilation angle	(Malm, 2009)
σ_{b0}/σ_{c0}	1.16	Ratio of biaxial to uniaxial compressive	(ABAQUS, 2012); (Lubliner et al., 1989)
K_c	0.7	Second stress invariant ratio	(ABAQUS, 2012)
μ	0.00025	Viscosity	(ABAQUS, 2012)
Elasticity	$\upsilon = 0.2$	Poisson's ratio for concrete members	Widely utilized in FEM simulations
	$\upsilon = 0.15$	Poisson's ratio for concrete masonry unit	
	$E_o = 4700\sqrt{\sigma_c'}$	Young's modulus	acc. (ACI, 2011)

For the tension behavior of concrete, the idealized stress-strain curve (Figure 4) based on Beshir (2016) was used to make the numerical analysis much more stable. Tensile stress, in general, increased in a form of a straight line with increasing the tensile strain to concrete cracking. After that, tensile stress reduced to zero in a form of a straight line. The calculation of the tensile strength σ_{ct} of concrete is equivalent to 10% of compressive strength (Darwin et al., 2016).

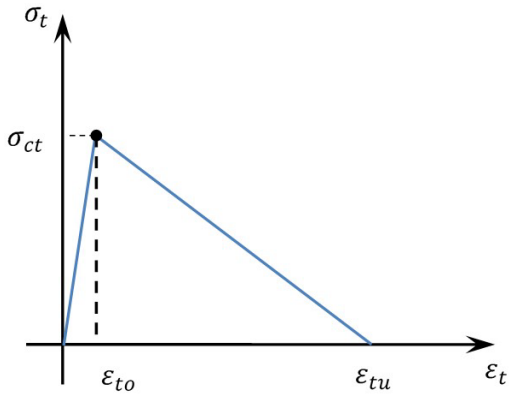

Figure 4. The stress-strain curve of concrete in tension.

The elastic region in the stress-strain curve of reinforcing rebar was modeled with typical values of 200,000 MPa, in addition to 0.3 for the modulus of Young and the ratio of Poisson, respectively. The plastic region has been defined following the specified test results provided by (Al-Chaar et al., 2002) by using the idealized curves as shown in Figure 5. The remainder key parameters were obtained based on Eurocode 3 (EN-1993-1-2, 2005b) provisions.

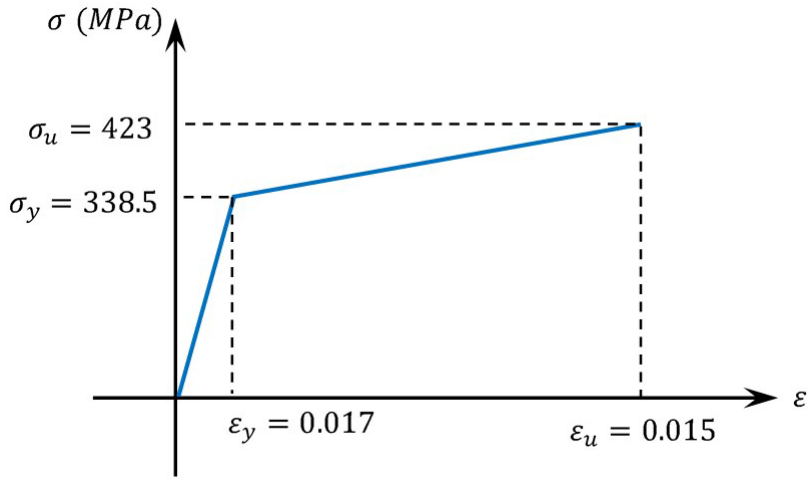

Figure 5. The idealized stress-strain curve for reinforcing rebars.

3.2. Joint interfaces elements

The masonry wall is a composite material, which comprises masonry units, as well as mortar joints as shown in Figure 6 (a). To achieve a complete masonry analysis, modeling all elements is necessary for masonry, including (masonry units and mortar, as well as masonry units, in addition to the mortar interface) as shown in Figure 6 (b). Based on this technique, masonry units, as well as mortar in joints can be modeled using continuum elements, while the unit-mortar interface can be modeled using interactive elements. Inelastic properties, the modulus of Young, and the ratio of Poisson must be considered for the masonry unit, as well as mortar alike. The interface involves the slip plane, in addition to the potential crack, along with initial stiffness to prevent the interpenetration of continuum (solid) elements (Laurenco et al., 1995). Accordingly, this allows for examining unit and mortar, as well as interface's combined action. This masonry model is costly, and it needs a long time to complete the analysis (Laurenco et al., 1995). Based on simplified micro-modeling (Figure 6 (c)), the masonry units were modeled using continuum (solid) elements. The mortar joints, as well as the masonry unit/mortar interface's behavior has been combined in a single interaction element as shown in Figure 7. The macro-modeling can be used by neglecting the variation between the masonry units, as well as the mortar joints by considering the masonry units, as well as the mortar joints' properties on average using the homogenization techniques (Laurenco et al., 1995), Figure 6 (d).

In this work, as shown in Figure 7, a simplified micro-modeling of the masonry has been utilized. Based on the utilized method, the masonry units are modeled by continuum (solid) elements. However, the mortar joints, as well as the masonry unit/mortar interface's behavior is united into a single interaction element.

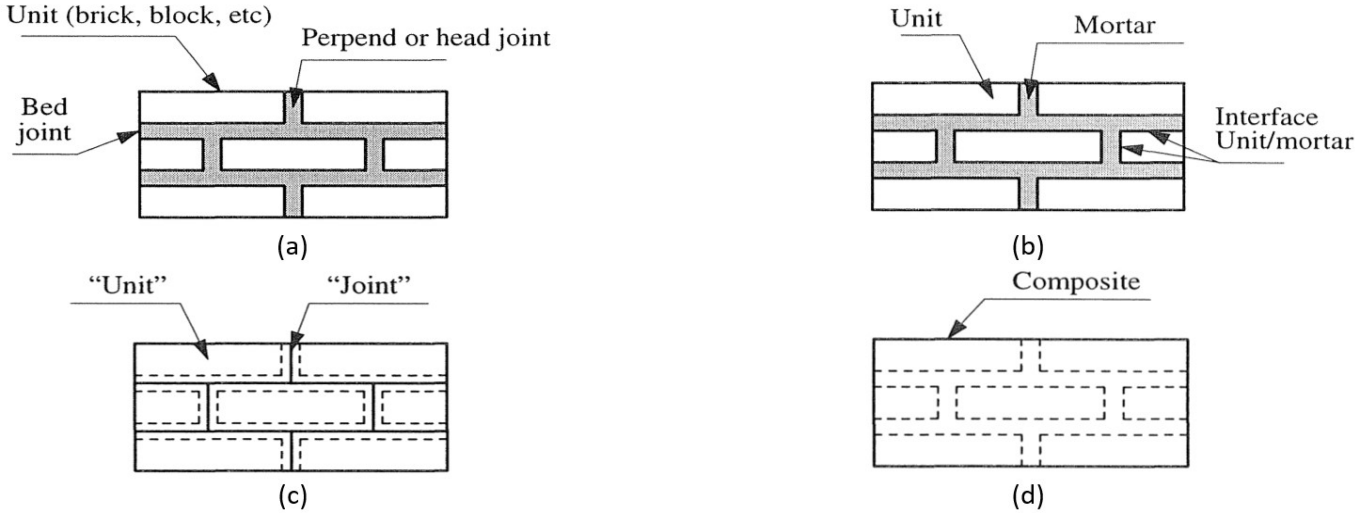

Figure 6. Modeling of the masonry structures (a) Masonry sample; (b) Detailed micro-modeling; (c) Simplified micro-modeling; (d) Macro-modeling (Laurenco et al., 1995)

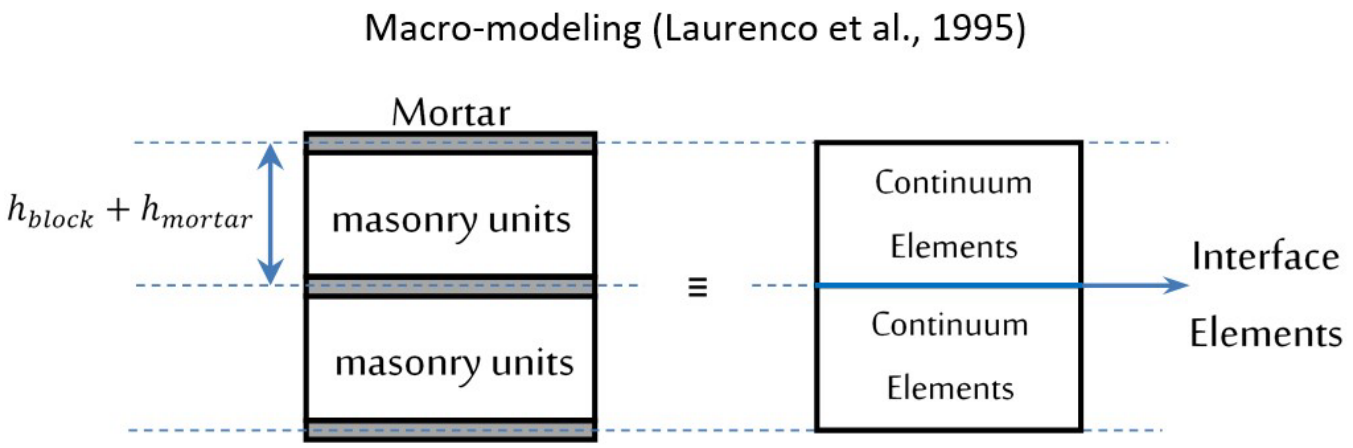

Figure 7. Basic micro-modeling modeling of the masonry structures using zero thickness elements (Laurenco et al., 1995)

3.3. Constraints and Interactions

The nodes of the truss elements (for reinforcing rebars) were constraining kinematically to the nodes of solid elements (concrete parts) via a fully embedded region algorithm. In addition, traditional node-to-surface discretization, as well as the approach of the small sliding tracking has been utilized to model interaction, which resulted from mortar located amid the block units. Moreover, to define the friction model between the contact surfaces, the coefficient of friction amid the units of the concrete masonry is equivalent to 0.44.

In ABAQUS, cohesive behavior is referred to as a fragment of interaction properties assigned to contact surfaces. In ABAQUS, the interface elements' properties can be identified based on the characteristics of the mortar and masonry unit of the experimental test conducted by Al-Chaar et al. (2002). The normal and shear stiffness (in first and second directions), which are essential for defining the mortar joints, as well as the masonry unit, and the mortar interface's behavior, are described in Eq. (5), and (6) (Lourenço, 1994). The normal, and shear stiffness (in first and second directions) value are shown in Table 4.

$$k_{nn} = \frac{E_u E_m}{h_m(E_u - E_m)} \tag{5}$$

$$k_{ss} \; and \; k_{tt} = \frac{G_u G_m}{h_m(G_u - G_m)} \tag{6}$$

where k_{nn}, k_{ss}, and k_{tt} are joint stiffness for the normal direction and first shear direction, as well as second shear direction, correspondingly, E_u and E_m are Young's modulus for masonry unit, as well as mortar, respectively, G_u and G_m represent the shear modulus of the masonry unit, in addition to the mortar, correspondingly, while h_m signifies the joints' actual thickness.

Table 4. Interface elements properties for the mortar

k_{nn} (MPa/mm)	$k_{ss} = k_{tt}$ (MPa/mm)
16020	11856

3.4. Boundary conditions and Loading application

Figure 8 shows the details of the boundary conditions and loading application. The vertical loads are divided into two parts, including the dead loads and the live load. The dead loads, including the members' self-weight, are identified in ABAQUS via the addition of density to the entire materials' definition. Thus, the finishing load, as well as the live load assumed are equal to (2 kN/m^2) according to ASCE (2010), Figure 8 (a).

The over-all loading on slabs is calculated following the ACI 318M-11 (ACI, 2011) equals 5.6 kN/m^2 (5.6*10-3 N/mm2). Because the modeling of the entire structure (3-story) needs a large high number of finite elements, and because of the available resources, not the entire structure can be modeled. Consequently, to reduce the considerable computational power and analyze running time, the 2-story RC frame structures were modeled in ABAQUS. However, loads at the top of second-floor columns that serve as third-floor loads as displayed in Table 5, and Figure 8 (b). The

column ends may be assumed to be fixed (Figure 8 (c)) for all the translational (U) and rotation (UR) in all the directions (i.e., Ux, Uy, Uz, URx, URy, and URz were restrained) at the bottom surfaces of the external columns to restrain the frames and reaction forces measurement.

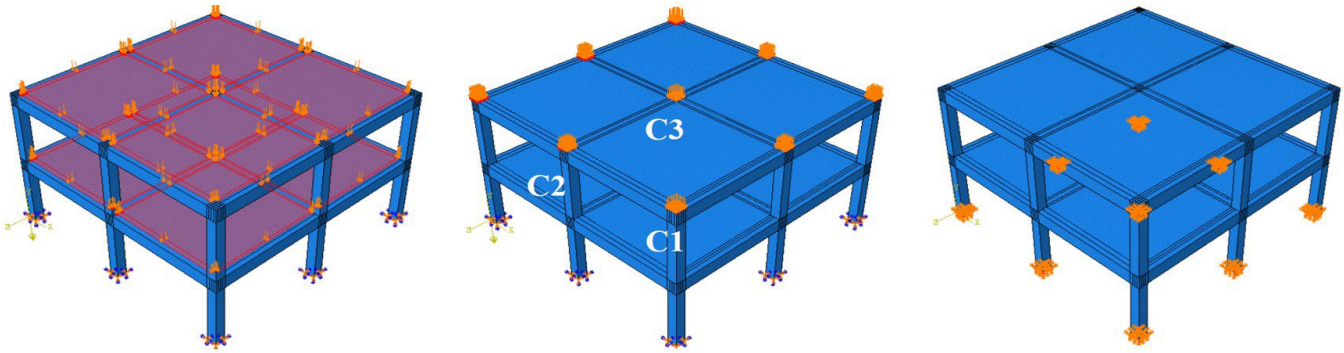

Figure 8. Boundary conditions and Loading application (a) Loads on the slabs; (b) Loads on the columns; (c) Boundary conditions.

Table 5. The loads on columns

Columns	Load	Pressure
Corner column (C1)	98.2 kN	0.62 N/mm^2
Edge column (C2)	222.4 kN	1.39 N/mm^2
Middle column (C2)	489 kN	3.056 N/mm^2

4 Verification of Finite Element Models

To achieve verification of the model of finite element, the masonry-infilled RC frames, which were tested to investigate the load-deflection response by Al-Chaar et al. (2002), were selected as the object of verification. The infilled frame was set up following the simulation techniques that are discussed in section 3 of this study. In ABAQUS, the model of a 3D finite element of the infilled frame was erected as displayed in Figure 9 (a). The beam, columns, masonry unit, and boundary conditions were constructed with the same as the experimental specimens' tests (Al-Chaar et al., 2002). Figure 9 (b) shows the mesh size, which was chosen to provide the most convergence and accurate results in comparison with the experimental results and reduces the required computational time at the same time. Figures 10 and 11 display a comparison between the simulation results of the finite element and the experimental results. As is shown in Figure 11, there is a very good agreement between the numerical results compared to the experimental test data, thereby it can be used in the analysis of progressive collapse scenarios of a frame structure.

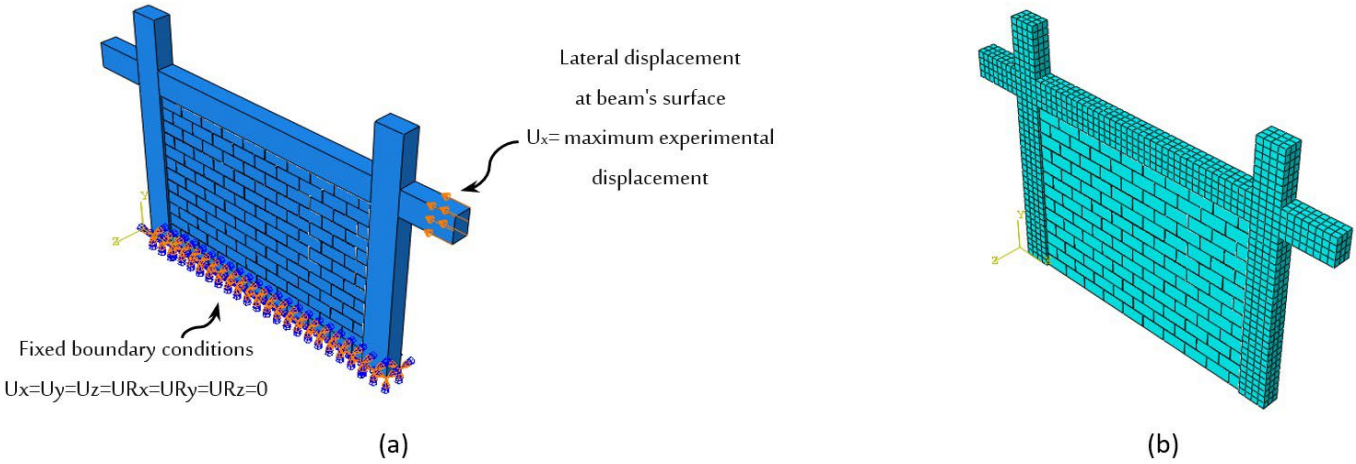

Figure 9. ABAQUS model of all frames (a) 3D model of the finite element of the infilled frame; (b) Element meshing

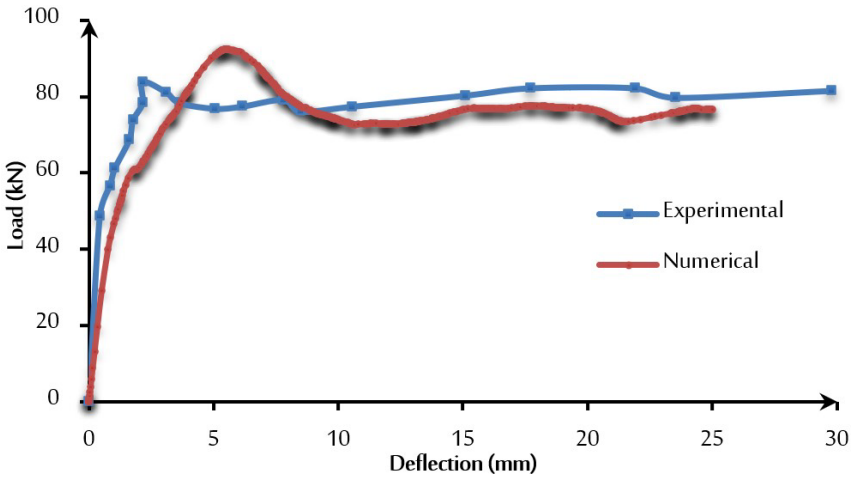

Figure 10. A comparison between the finite element infilled frame vs. the experimental infilled frame

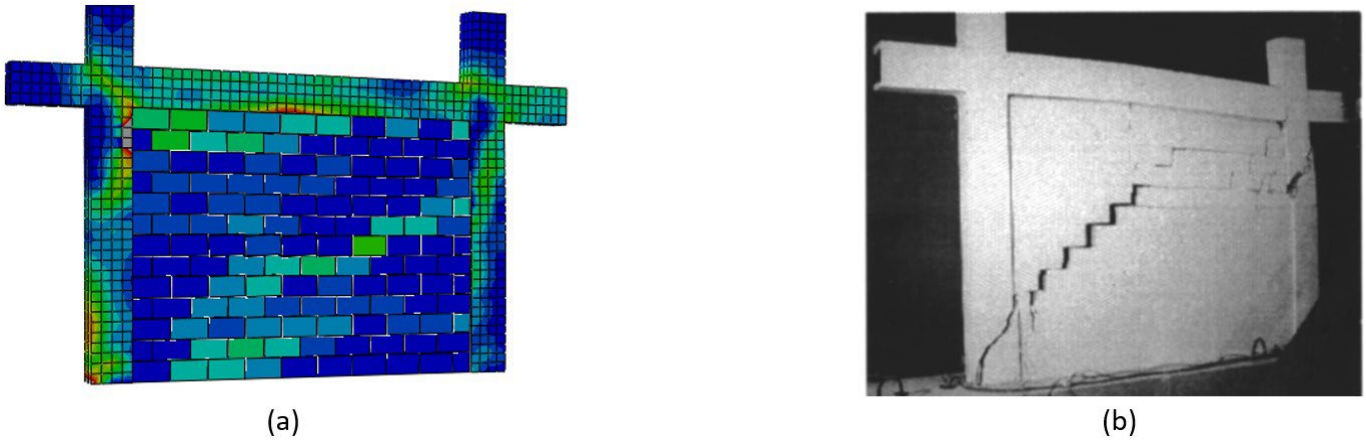

Figure 11. A comparison between deformed shapes (a) The finite element infilled frame, and (b) The experimental infilled frame (Al-Chaar et al., 2002)

5. Progressive Collapse Scenarios analysis

The effect of extreme events (e.g. impact and blast) on the structures is a dynamic influence. For designers, checking the structure, whether it efficiently absorbs the removed column impact, in addition to preventing progressive collapse, is essential via the ability of bridging loads over the removed column. The DoD (2010) and GSA (2003) includes analyzing the behavior of structures under different column removal scenarios to simulate the local damage by assuming that the column had been lost through extreme events. This utilized method has been implemented by researchers (Xiao et al., 2015, Almusallam et al., 2018, Alshaikh et al., 2019, Alshaikh et al., 2020, Qian et al., 2020b, Qiang et al., 2020, Qiu et al., 2020, Vieira et al., 2020). The list of the progressive collapse scenarios analysis considered in this study is illustrated in Table 6. It should be noted that the columns in perimeter bays of the first story are vulnerable, especially to destruction by car bombs or truck bombs; the largest loads are carried by these columns as opposed to the remaining floors. For this reason, the columns on the first floor were removed. The infill walls were only created in second-floor frames in order to examine the impact of infill walls on progressive collapse.

Table 6. Progressive collapse scenarios

Case	Infilled walls type	Member removed
1	Full-height infill walls	Corner, Edge, and Middle columns
2	Infill walls with openings (three openings ratios 12%, 17%, and 28%)	Corner, Edge, and Middle columns
3	Partial infill walls (three reductions ratios of infill 12%, 16%, and 28%)	Corner, Edge, and Middle columns

5.1. Case 1- Full-Height Infill Walls

Vertical displacement has been studied for the node, which is positioned right above the removed column to examine the infilled frames' impact on the progressive collapse. The deformation shape, as well as the vertical displacements of both cases, i.e., the buildings with/without the infill walls, for the removal of the corner column, the edge column, as well as the middle column, is displayed in Figure 12. As demonstrated in Figure 12 and Table 7, utilizing the infill walls on the structure reduced the vertical displacement in the removed-column regions from 40 to 80%. If the middle column is removed based on Figure 12(c) and Table 7, the maximum vertical displacement of the entire 3 scenarios has been achieved, but the smallest vertical displacement has been recorded when the corner column is removed as shown in Figure 12 (a) and Table 7.

Table 7. Comparison between maximum vertical displacements

Member removed	Maximum vertical displacement, (mm)		
	building without infill walls	building with infill walls	% Relative Variation
Corner column	12.437	6.451	+48%
Edge column	31.863	6.640	+79%
Middle column	236.294	44.621	+81%

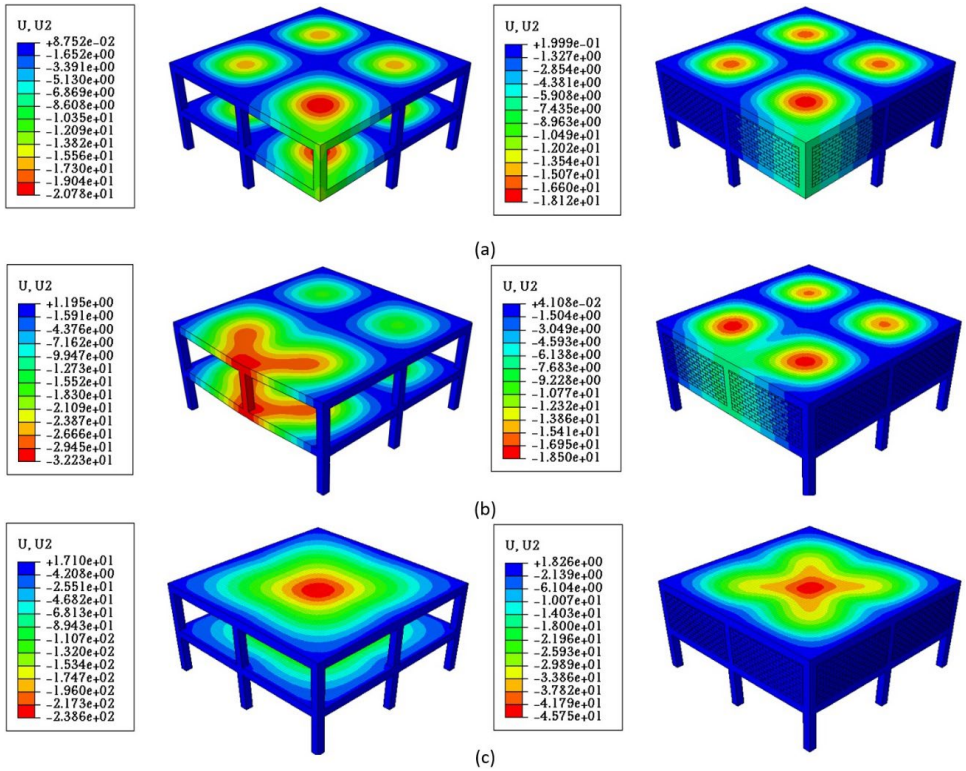

Figure 12. The deformation shape, as well as the vertical displacements of both cases, including (a) The corner column removal; (b) The edge column removal; (c) The middle column removal.

5.2. Case 2- Infill Walls with Openings

The opening has been made in the middle of the walls. Different dimensions of the openings reliant on the walls' dimensions (12%, 17%, and 28%). The sudden removal of the following columns has been carried out (the edge column, the edge column, as well as the middle column). The openings' impact on progressive collapse has been examined.

Corner Column Removal

Vertical displacement has been studied of the node, which is positioned right above the removed corner column to examine the impact on progressive collapse. Figure 13 displays the given deformation shape, as well as vertical displacements of the buildings with the infill walls when the corner column is removed. The resulting reduction ratios are shown in Figure 14. If small openings exist in infill walls (12%, 17%), this would provide further frames' ductility; the capacity of the frame has been improved vs. the full-height infilled frame because of the frame's changing placements struts.

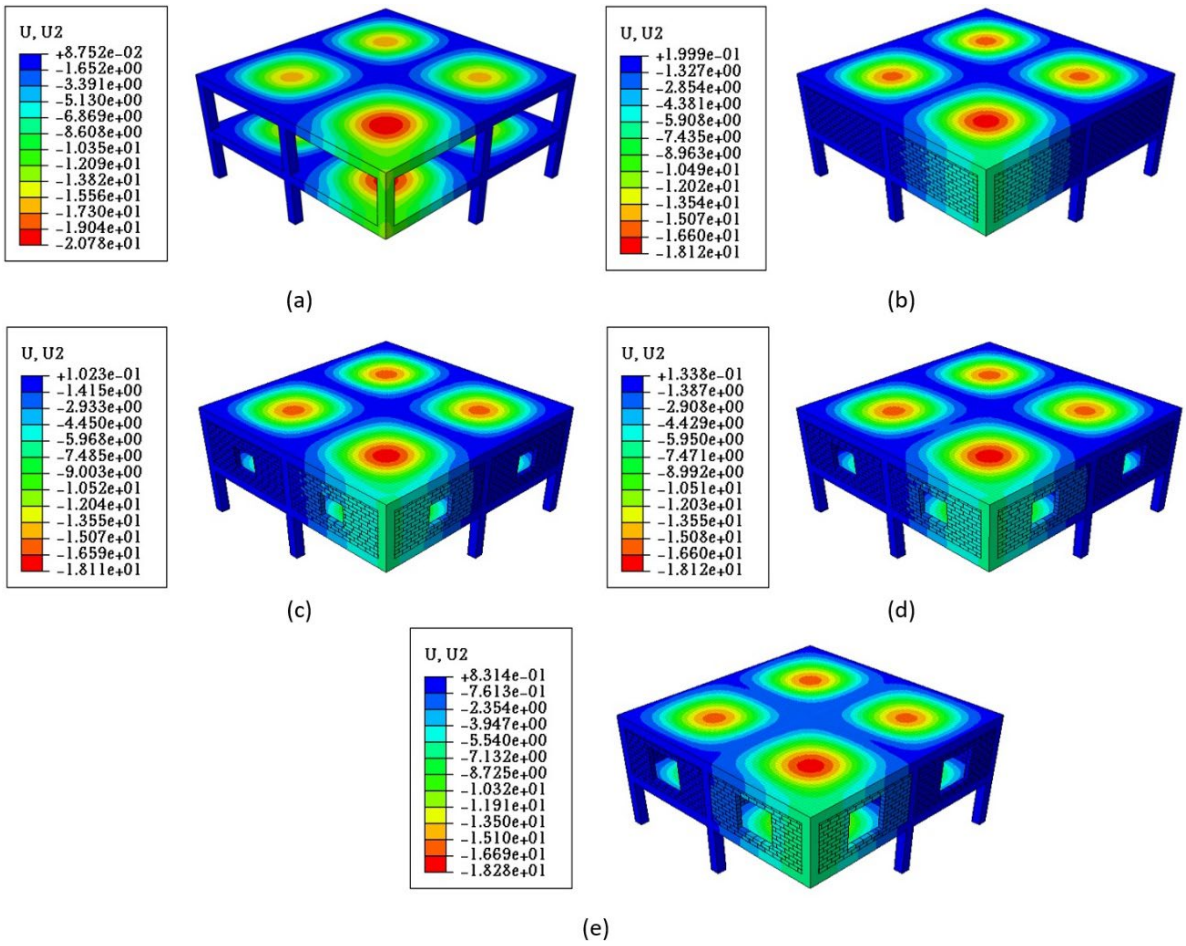

Figure 13. The deformation shape, as well as the vertical displacements- corner column removal (a) Bare building; (b) Infilled building; (c) 12% Opening; (d) 17% Opening; (e) 28% Opening.

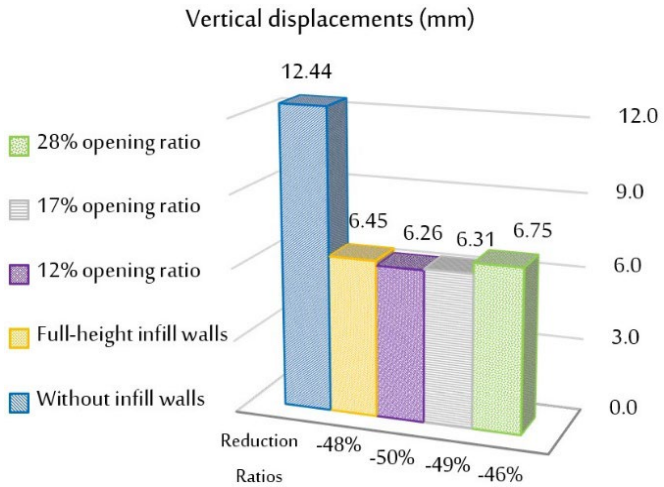

Figure 14. The summary vertical displacements for openings in the infilled frame - corner column removal.

Edge Column Removal

Based on Figure 15, the deformation shape, as well as the vertical displacements are shown for the buildings with the infill walls in the edge column removal. Figure 16 displays the obtained reduction ratios. If small openings exist in infill walls (12%), this would provide further frames' ductility; the capacity of the frame has been improved vs. the full-height infilled frame. It has also been shown that if large openings exist (17%, 28%), this would reduce the infill walls' capacity vs. the full-height infilled frame. This can be attributed to reducing the infill walls' performance due to the strength loss because of openings. This goes in line with the results obtained from the corner column removal.

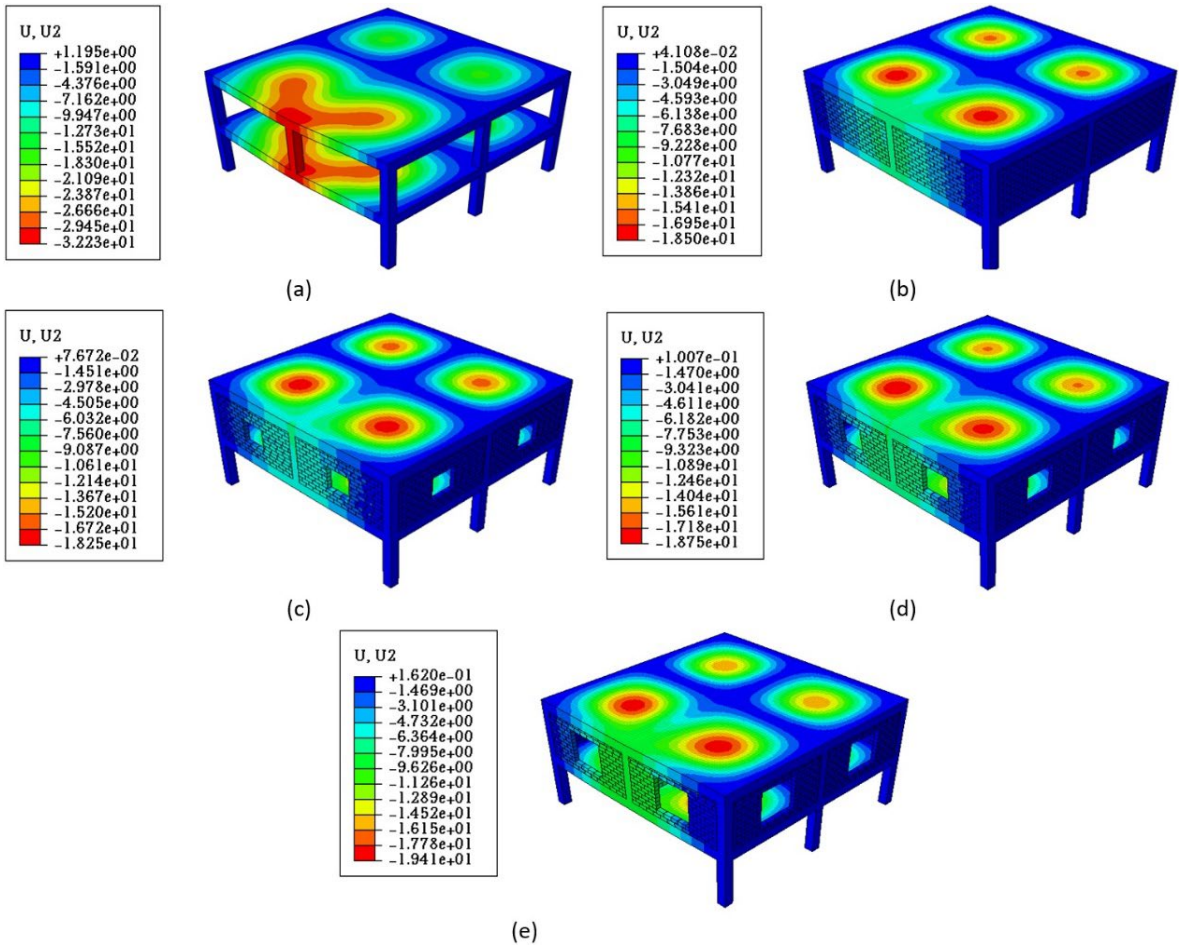

Figure 15. The deformation shape, as well as the vertical displacements-edge column removal (a) Bare building; (b) Infilled building; (c) 12% Opening; (d) 17% Opening; (e) 28% Opening.

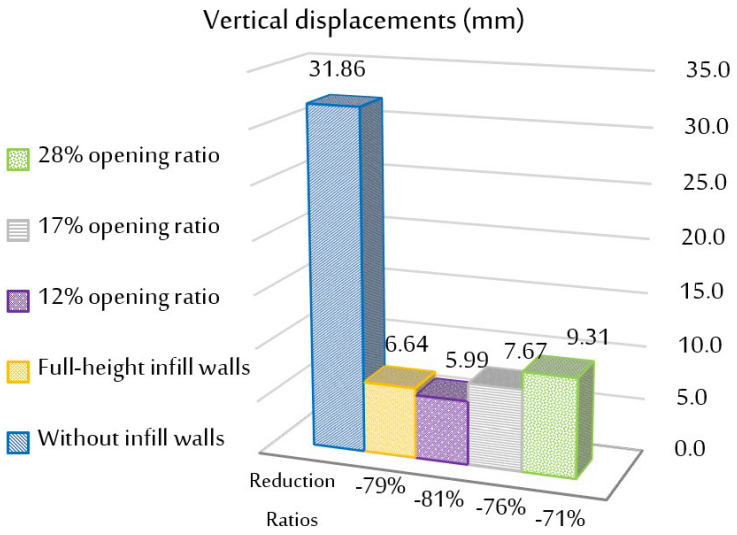

Figure 16. The summary of the vertical displacements of the openings in the infilled frame- edge column removal.

Middle Column Removal

Figure 17 displays the deformation shape, as well as the vertical displacements of the buildings with the infill walls, and Figure 18 displays the obtained reduction ratios. No remarkable difference was observed if the openings exist in infill walls with these proportions of (12%, 28%). Based on the results, when the openings existed (17%), this provided further frames' ductility, thereby improving the capacity of the frame vs. the full-height infilled frame.

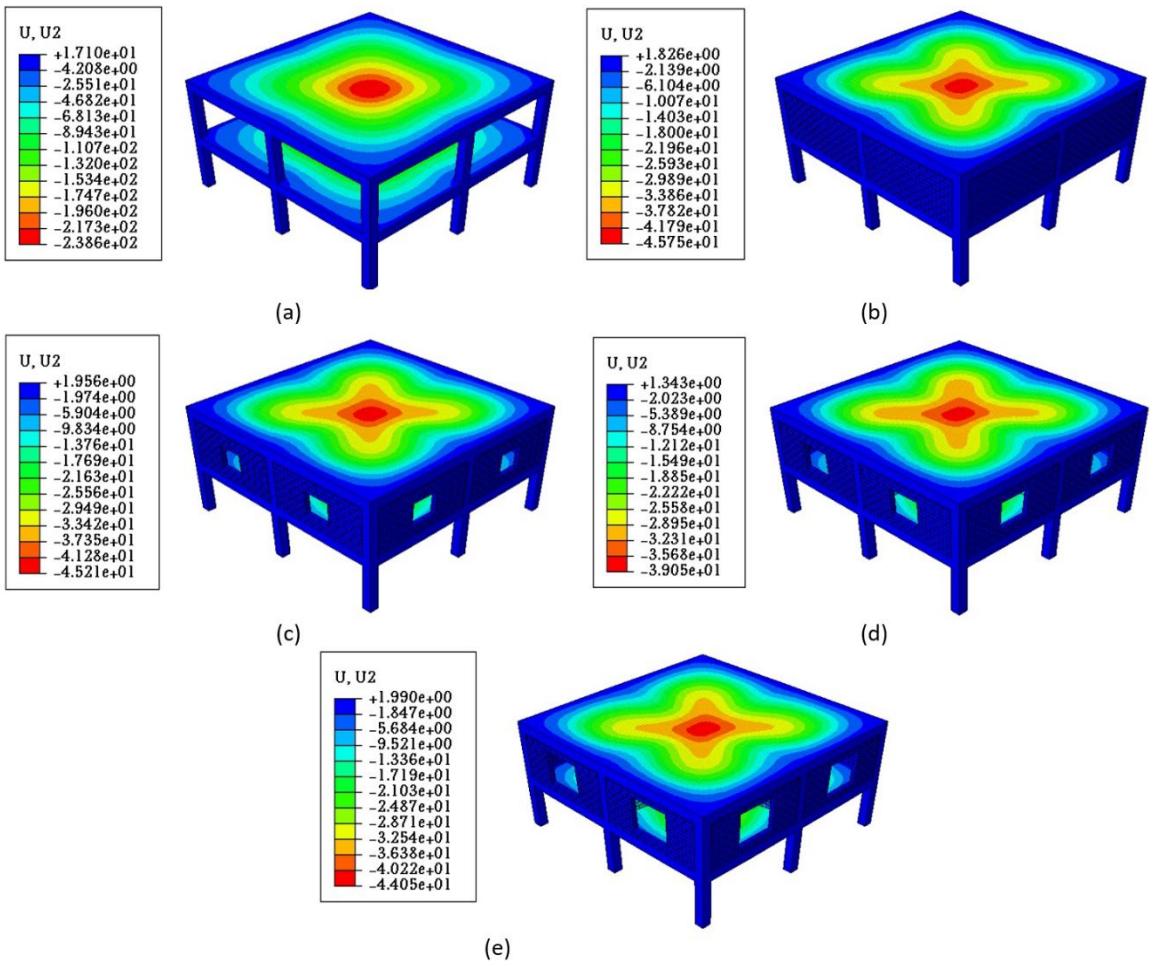

Figure 17. The deformation shape, as well as the vertical displacements-middle column removal (a) Bare building; (b) Infilled building; (c) 12% Opening; (d) 17% Opening; (e) 28% Opening.

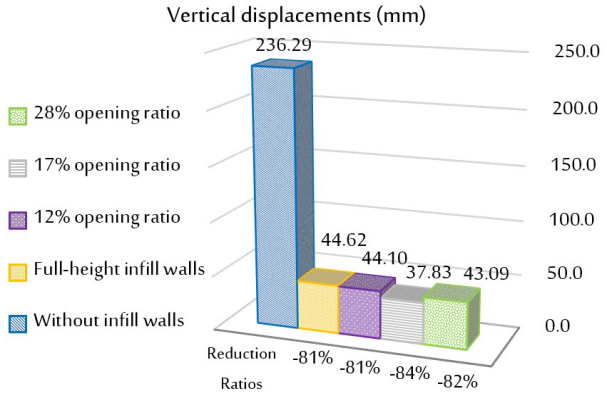

Figure 18. The summary of the vertical displacements of the openings in the infilled frame-middle column removal.

5.3. Case 3- Partial Infill Walls

The opening has been made upward in the walls, and different dimensions of openings were reliant on the walls' dimensions (12%, 16%, and 28%). The sudden removal of the corner columns took place. The openings' impact on progressive collapse has been examined. The vertical displacement has been studies regarding the node right above the removed corner column in order to examine the impacts on progressive collapse. Figure 19 displays deformation shape, as well as vertical displacements of partially infill walls' buildings when the corner column is removed. Figure 20 displays the obtained reduction ratios. No prominent difference was, accordingly, observed when the partly infill frame with an opening exists (12%, 16%), and infill walls performed less efficiently vs. the full-height infilled frame.

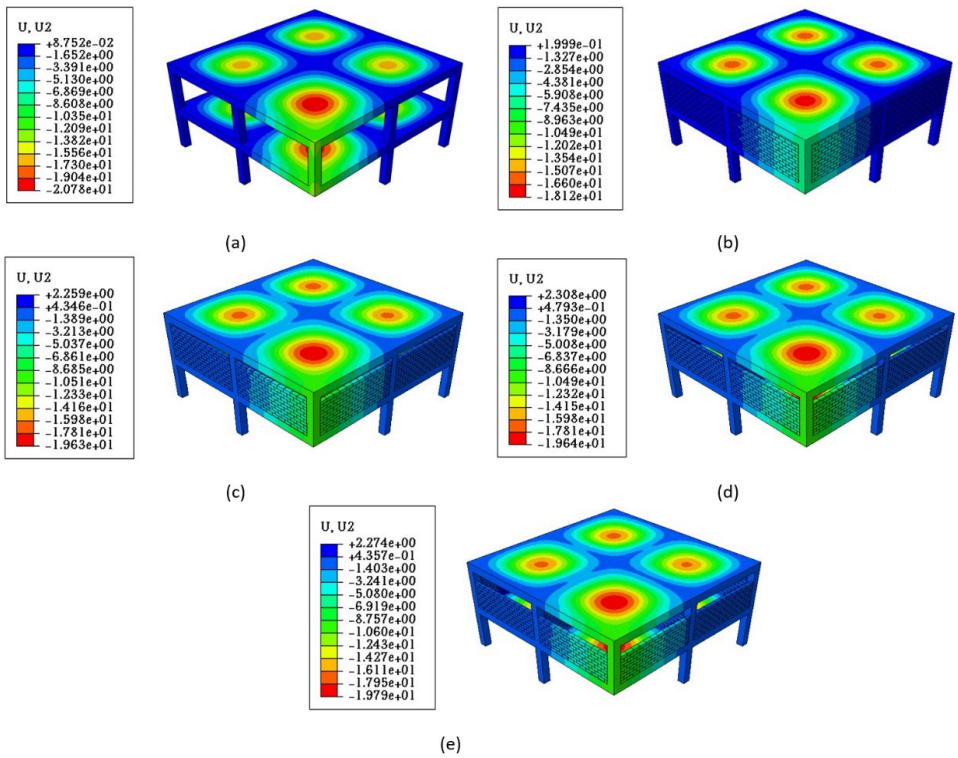

Figure 19. The deformation shape, as well as the vertical displacements of the partially infilled frame-corner column removal (a) Bare building; (b) Infilled building; (c) 12% Opening; (d) 16% Opening; (e) 28% Opening.

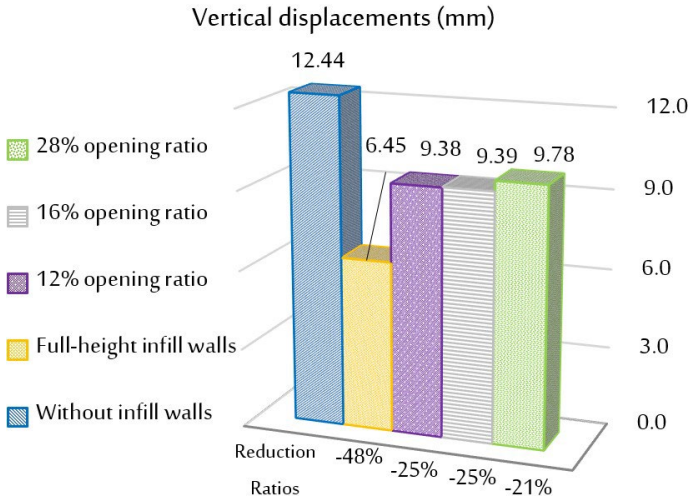

Figure 20. The summary of the vertical displacements of the partly infilled frame-corner column removal.

5.4. Analysis and discussion of results

The infill walls' contribution in the mechanism of progressive collapse has been represented through a diagonal strut, which was formed in walls (see Figure 21) and can provide additional resistance and, meanwhile, modifying the distribution of the internal forces on of RC frames members. The width of the diagonal strut reliant on the infill's relative flexural stiffness to that of the columns' stiffness in the confining frame. Based on Figure 21, the schematic of expected equivalent compressive strut locations of the infill walls in RC frames is displayed under scenarios of progressive collapse (Al-Chaar et al., 2002, Shan et al., 2019, Yu et al., 2019). Based on every situation, the infill wall functioned as a number of closely separate solid parts (e.g., if the openings, as well as the partial infill, exist). The main compressive stresses were developed lengthwise the diagonal area of every solid part via interacting with confining frame members, as well as infill walls (i.e., the so-called truss mechanism). This is clearly shown by the grey arrows in the provided figure. Therefore, the infill walls have the capability of redistributing column removal loading and, thereby, preventing progressive collapse or mitigating it.

Regarding full-height infill walls and based on Figure 21 (a), the applied vertical load transfer was implemented by using the axial compression lengthwise the diagonal strut of each of the wall panels due to small beams stiffness, which is quite smaller compared to the wall's stiffness. Also, the shear stress distribution concentrated in the diagonal compressive strut region's ends, i.e., interfaces (displayed by the blue and red arrows in Figure 21) round the first-story beam's adjacent end, as well as the second-story beam's remote end, whereby the two beams function like tension chord. In comparison, the presence of openings changed the distribution of shear stress due to detachment of the concrete masonry units from the beams round the opening with increasing the vertical displacement according to Figure 21 (b).

When small openings exist in infill walls (12%, 17%), this provided further frames' ductility, thereby improving the capacity of the frame as opposed to the full-height infilled frame. This can be attributed to changing the struts' location in the given frame based on Figure 21 (b). The equivalent strut was expected to behave in a similar manner to the full-height infilled frame. The results revealed that when large openings exist (28%), this would reduce the infill walls' capacity vs. the full-height infilled frame. This can be attributed to the infill walls' reduced performance due to strength loss because of large openings. When the openings' area is equivalent, or it is larger than 60% of the infill walls' area. Accordingly, the infill walls' impact should be ignored (Al-Chaar et al., 2002).

The reason behind reducing the partly infilled frame's capacity can be attributed to reducing the wall's length interaction with confining frame members, as shown in Figure 21 (c). This has reduced the corresponding strut width and, thereby, reducing the capacity of the partly infill walls significantly compared to the full height infills walls' capacity.

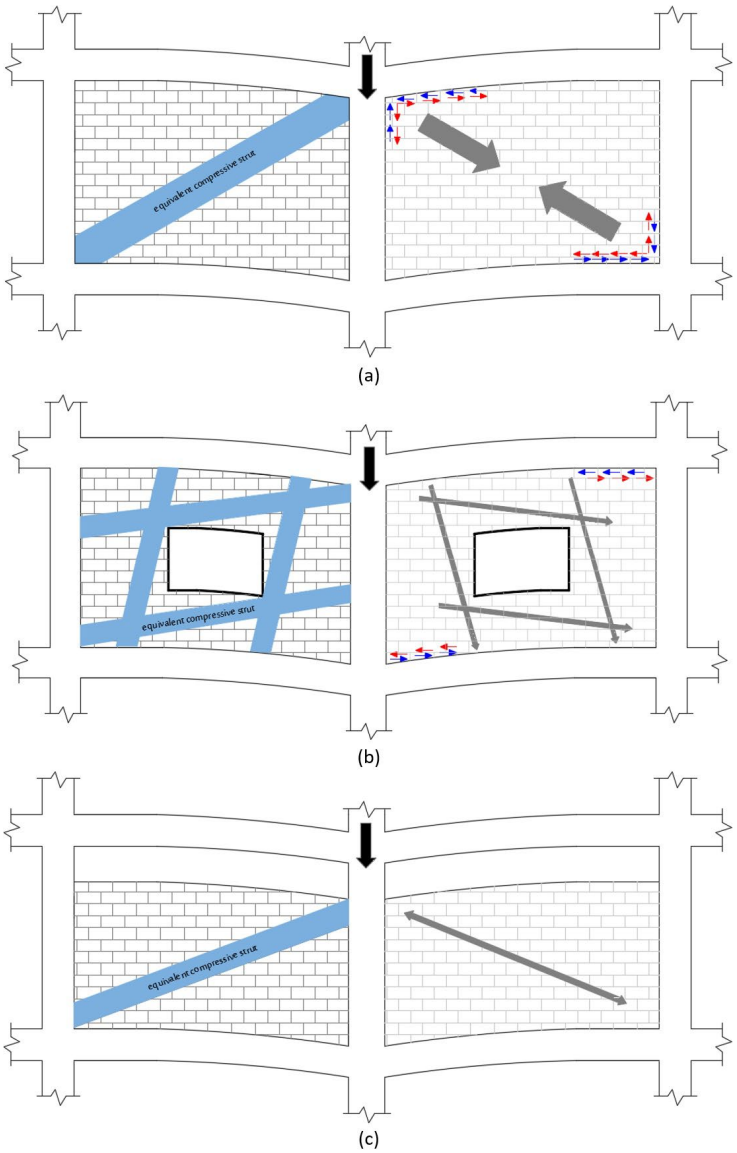

Figure 21. Possible strut locations for infill walls (a) Full-height infill; (b) Infill with openings; (c) Partial infill (Al-Chaar et al., 2002, Shan et al., 2019, Yu et al., 2019)

6. Conclusion

This study examined the effect of infilled frames and investigated the effects of variables parameters (i.e., the openings' percentage in infill walls - several columns removal on the 1st floor - partial infilled) in RC structures, subject to scenarios of progressive collapse. Based on the results, several observations were provided and a number of conclusions were advanced as follows:

1. The finite element model has the capability of predicting the masonry-infilled RC frames' behavior, which achieved good accuracy in contrast with the authors' experimental results of Al-Chaar et al. (2002).
2. The infill walls' impact through the frame's design procedure should be considered as it exerts a considerable impact on the resistance of progressive collapse. Based on the results, the reduction ratios in the vertical displacement in the regions of the removed columns are expected to reach 80%.
3. When small openings in the core of the infill walls exist, this provided further frames' ductility as opposed to the full-height infilled frame due to changing placement of struts in the frame. Therefore, when openings are necessary for the walls, it is preferred to carry out in small ratios and stay away from the struts place.
4. Regarding the large openings, the results showed that there is a reduction in the capacity of infill walls with openings compared with the full-height infilled frames. This can be attributed to the infill walls' reduced performance due to the strength loss because of the large openings.
5. No prominent difference has been observed when the partly infill frame with the opening exists (12%, 16%). According to the results, the reduced percentage in vertical displacement is expected to reach 25%.

The researchers believe that further investigations should be conducted so that different techniques are identified to enhance current buildings. This would improve the performance against the progressive collapse. The effect of column removal from the upper floors should be examined. The removal effect of multi-columns on the same floor should be also investigated.

ACKNOWLEDGEMENTS

The authors extend their appreciation to Researchers Supporting Project number (RSP-2021/343), King Saud University, Riyadh, Saudi Arabia.

Author's Contribuitions: Conceptualization, IMH Alshaikh; Methodology, IMH Alshaikh, and A Abadel; Writing - original draft, IMH Alshaikh, and M Nehdi; Writing - review & editing, IMH Alshaikh, and H Alghamdi; Funding acquisition, A Abadel; Resources, A Abadel, and A Altheeb.

Editor: Marcílio Alves.

References

Abaqus (2012) User Assistance. Dassault Systèmes Simulia Corporation, Providence, Rhode Island, USA.

Abdulla, K. F., Cunningham, L. S. & Gillie, M. (2017) Simulating masonry wall behaviour using a simplified micro-model approach. Engineering Structures 151:349-365.

ACI (2011) Building code requirements for structural concrete and commentary.

Al-Chaar, G., Issa, M. & Sweeney, S. (2002) Behavior of masonry-infilled nonductile reinforced concrete frames. Journal of Structural Engineering 128(8):1055-1063.

Almusallam, T. H., Elsanadedy, H. M., Al-Salloum, Y. A., Siddiqui, N. A. & Iqbal, R. A. (2018) Experimental Investigation on Vulnerability of Precast RC Beam-column Joints to Progressive Collapse. KSCE Journal of Civil Engineering 22(10):3995-4010.

Alshaikh, I. M., Bakar, B. A., Alwesabi, E. A. & Akil, H. M. (2019) Progressive collapse of reinforced rubberised concrete: Experimental study. Construction and Building Materials 226:307-316.

Alshaikh, I. M., Bakar, B. A., Alwesabi, E. A. & Akil, H. M. (2020) Experimental investigation of the progressive collapse of reinforced concrete structures: An overview. In Structures.) Elsevier, vol. 25, pp. 881-900.

Asce (2010) American Society of Civil Engineers - Minimum design loads and associated criteria for buildings and other structures.) ASCE Reston, VA.

Barros, M., Cavaco, E., Neves, L. & Júlio, E. (2019) Effect of non-structural masonry brick infill walls on the robustness of a RC framed building severely damaged due to a landslide. Engineering Structures 180:274-283.

Beshir, M. a. E. Z. (2016) Robustness of Composite Framed Structures in Fire. The University of Manchester (United Kingdom).

Darwin, D., Dolan, C. W. & Nilson, A. H. (2016) Design of concrete structures. McGraw-Hill Education New York.

Daryan, A. S., Ziaei, M., Golafshar, A., Pirmoz, A. & Assareh, M. A. (2009) A study of the effect of infilled brick walls on behavior of eccentrically braced frames using explicit finite elements method. American J. of Engineering and Applied Sciences 2(1):96-104.

Dod (2010) Design of buildings to resist progressive collapse. Unified Facilities Criteria (UFC) 4-023-03.

EN-1992-1-1 (2005a) Eurocode 2: Design of Concrete Structures: General Rules and Rules for Buildings and Structural Fire Design. Thomas Telford.

EN-1993-1-2 (2005b) Eurocode 3: Design of Steel Structures-Part 1-2: General Rules-Structural Fire Design. London: European Committee for Standardisation.

Eren, N., Brunesi, E. & Nascimbene, R. (2019) Influence of masonry infills on the progressive collapse resistance of reinforced concrete framed buildings. Engineering Structures 178:375-394.

Gsa (2003) Progressive collapse analysis and design guidelines for new federal office buildings and major modernization projects. Washington, DC.

Ibrahim Al-Shaikh, N. F. (2014) Numerical Analysis of Masonry-Infilled Reinforced Concrete Frames. Journal of Science and Technology 19 (2):21-28.

J. Centeno, C. E. V., S. Foo (2008) SHAKE TABLE TESTING OF GRAVITY LOAD DESIGNED REINFORCED CONCRETE FRAMES WITH UNREINFORCED MASONRY INFILL WALLS. The 14th World Conference on Earthquake Engineering.

Laurenco, P., Rots, J. G. & Blaauwendraad, J. (1995) Two approaches for the analysis of masonry structures: micro and macro-modeling. HERON, 40 (4), 1995.

Lee, J. & Fenves, G. L. (1998) Plastic-damage model for cyclic loading of concrete structures. Journal of engineering mechanics 124(8):892-900.

Li, S., Shan, S., Zhai, C. & Xie, L. (2016) Experimental and numerical study on progressive collapse process of RC frames with full-height infill walls. Engineering Failure Analysis 59:57-68.

Lourenço, P. (1994) Analysis of masonry structures with interface elements. Rep. No. 03-21-22-0 1.

Lubliner, J., Oliver, J., Oller, S. & Oñate, E. (1989) A plastic-damage model for concrete. International Journal of solids and structures 25(3):299-326.

Lupoae, M., Baciu, C., Constantin, D. & Puscau, H. (2011) Aspects concerning progressive collapse of a reinforced concrete frame structure with infill walls. In World Congress on Engineering.), vol. 3.

Malm, R. (2009) Predicting shear type crack initiation and growth in concrete with non-linear finite element method.) KTH.

Qian, K., Lan, D.-Q., Fu, F. & Li, B. (2020a) Effects of infilled wall opening on load resisting capacity of RC frames to mitigate progressive collapse risk. Engineering Structures 223:111196.

Qian, K., Liang, S.-L., Feng, D.-C., Fu, F. & Wu, G. (2020b) Experimental and numerical investigation on progressive collapse resistance of post-tensioned precast concrete beam-column subassemblages. Journal of Structural Engineering 146(9):04020170.

Qiang, H., Yang, J., Feng, P. & Qin, W. (2020) Kinked rebar configurations for improving the progressive collapse behaviours of RC frames under middle column removal scenarios. Engineering Structures 211:110425.

Qiu, L., Lin, F. & Wu, K. (2020) Improving progressive collapse resistance of RC beam–column subassemblages using external steel cables. Journal of Performance of Constructed Facilities 34(1):04019079.

Sasani, M. (2008) Response of a reinforced concrete infilled-frame structure to removal of two adjacent columns. Engineering Structures 30(9):2478-2491.

Sasani, M. & Kropelnicki, J. (2008) Progressive collapse analysis of an RC structure. The Structural Design of Tall and Special Buildings 17(4):757-771.

Shan, S., Li, S., Kose, M. M., Sezen, H. & Wang, S. (2019) Effect of partial infill walls on collapse behavior of reinforced concrete frames. Engineering Structures 197:109377.

Shan, S., Li, S., Xu, S. & Xie, L. (2016) Experimental study on the progressive collapse performance of RC frames with infill walls. Engineering Structures 111:80-92.

Vieira, A. D. A., Triantafyllou, S. & Bournas, D. (2020) Strengthening of RC frame subassemblies against progressive collapse using TRM and NSM reinforcement. Engineering Structures 207:110002.

Woodson, S. & Baylot, J. (2000) Quarter-scale building/column experiments. In Structures Congress 2000- Advanced Technology in Structural Engineering.), vol. 2000.

Xiao, Y., Kunnath, S., Li, F., Zhao, Y., Lew, H. & Bao, Y. (2015) Collapse Test of Three-Story Half-Scale Reinforced Concrete Frame Building. ACI Structural journal 112(4).

Yu, J., Gan, Y.-P., Wu, J. & Wu, H. (2019) Effect of concrete masonry infill walls on progressive collapse performance of reinforced concrete infilled frames. Engineering Structures 191:179-193.